

Photoionization and recombination of Fe XIX

Hong Lin Zhang¹ and Anil K. Pradhan²

¹*Applied Theoretical and Computational Physics Division, Los Alamos National Laboratory, Los Alamos, NM 87545, USA*

²*Department of Astronomy, The Ohio State University, Columbus, OH 43210, USA*

Accepted xxxxxx Received xxxxxx; in original form xxxxxx

ABSTRACT

Photoionization cross sections and recombination rate coefficients are presented for the L-shell ground state fine structure levels $2s^22p^4\ ^3P_{2,0,1}$ of Fe XIX. Several sets of calculations including relativistic effects are carried out: (i) Breit-Pauli R-matrix (BPRM), (ii) Relativistic Distorted Wave (RDW), and (iii) a semi-relativistic calculation. Non-relativistic LS coupling calculations are also done for comparison. The BPRM calculations employ a configuration interaction target representation for Fe XX consisting of 12 LS terms (23-fine structure levels), as in the recently reported BPRM calculations by Donnelly *et al.* (MNRAS, 307, 595, 1999). The background cross sections in all three sets of present calculations agree with one another, but differ considerably from those of Donnelly *et al.*. Owing to much more extensive resonance structures in the present BPRM calculations, the sum of the corresponding recombination rate coefficients for the $^3P_{2,0,1}$ levels are up to 50% higher than the LS rates at low temperatures but comparable for higher temperatures; in contrast to the results of Donnelly *et al.* who obtained the LS rates to be higher than their BPRM results by about a factor of 2. Reasons for these discrepancies are discussed.

Key words: Atomic Processes – Atomic Data – X-ray: L-shell

1 INTRODUCTION

Photoionization and recombination are fundamental atomic processes in astrophysical plasmas. However, rather elaborate and extensive atomic calculations are required in order to compute the related photoionization and recombination coefficients in an accurate and self-consistent manner. In most existing astrophysical models these atomic data are from methods that do not adequately consider the level of complexity attributable to the large number of autoionizing resonances that manifest themselves in the photoionization cross sections, and consequently, in the inverse process of (electron - ion) recombination. Most previous atomic calculations divide the recombination process into non-resonant ‘radiative recombination’ (RR) and resonant ‘di-electronic recombination’ (DR). This division is valid only if either RR or DR is dominant in a given energy region. In general, in the low energy region, the electron-ion recombination may contain significant contributions from both the autoionizing resonances and the background cross section. Therefore, an accurate theoretical treatment requires both the RR and DR to be treated in a unified manner. Recent developments enable such a unified and self-consistent calculation of photoionization and recombination cross sections, including highly detailed resonance structures, using the close coupling approximation and the R-matrix method (Nahar & Pradhan 1992, 1994; NP1 and NP2). For highly charged

ions, relativistic effects may be considered in the Breit-Pauli R-matrix (BPRM) approximation (Zhang & Pradhan 1997; Zhang, Nahar & Pradhan (ZNP) 1999). Electron-ion recombination rate coefficients are thereby obtained including the RR and DR processes through *ab initio* calculations.

In high temperature X-ray sources K- and L-shell atomic ions are prominent constituents. In particular the highly ionized ions of iron are important in laboratory and astrophysical sources (Liedahl *et al.* 1992). Recently, Donnelly *et al.* (1999) employed the BPRM approximation to calculate total and partial photoionization cross sections for the ground state fine structure levels $2s^22p^4\ ^3P_{2,0,1}$ of Fe XIX. They also calculated recombination rate coefficients for the transitions from the ground level $2s^22p^3\ ^4S_{3/2}$ in Fe XX to those levels in Fe XIX using the partial photoionization cross sections. They employed a sophisticated representation for the 12 lowest $SL\pi$ terms corresponding to 23 $J\pi$ fine structure levels in the target ion Fe XX. Donnelly *et al.* obtained fine structure photoionization cross sections for the three ground state levels such that the individual cross sections differed considerably from each other, in background and in details of resonances, and the weighted average differed from the non-relativistic LS values by more than a factor of two. The results were surprising since they imply relativistic effects are larger than expected. Otherwise, the individual fine structure cross sections should have a background of the same magnitude (although different res-

onance structures). For example, an earlier BPRM study on C-like Fe XXI, with the same ground state symmetries $^3P_{0,1,2}$ showed that the background cross sections for the three levels were nearly equal (Zhang 1998). We have therefore repeated the calculations of Donnelly *et al.* as precisely as possible, using the same eigenfunction expansion as in their work. We obtain very different results, confirmed by several other calculations in different approximations, as well as much smaller relativistic effects. New recombination rate coefficients for the Fe XIX ground levels are also presented and compared.

2 THEORY

The extension of the close coupling method to electron-ion recombination is described in earlier works (NP1, NP2, ZNP), together with the details of the unified treatment. Here we present a brief description of the theory relevant to the present calculations. The calculations are carried out in the close coupling (CC) approximation employing the R -matrix method, in LS coupling and in intermediate coupling with the BP Hamiltonian. The target ion is represented by an N -electron system, and the total wavefunction expansion, $\Psi(E)$, of the $(N+1)$ electron-ion system of symmetry $SL\pi$ (LS coupling) or $J\pi$ (BP, intermediate coupling) may be represented in terms of the target eigenfunctions as:

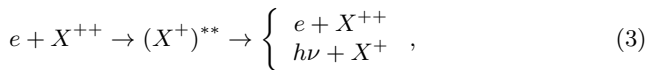
$$\Psi(E) = A \sum_i \chi_i \theta_i + \sum_j c_j \Phi_j, \quad (1)$$

where χ_i is the target wavefunction in a specific state $S_i L_i \pi_i$ or $J_i \pi_i$ and θ_i is the wavefunction for the $(N+1)$ -th electron in a channel labeled as $S_i L_i (J_i) \pi_i k_i^2 \ell_i (SL\pi$ or $J\pi)$; k_i^2 being its incident kinetic energy. Φ_j 's are the correlation functions of the $(N+1)$ -electron system that account for short range correlation and the orthogonality between the continuum and the bound orbitals. Most of the present calculations are in the BP approximation (Pradhan & Zhang 1997, Zhang 1998).

Recombination of an incoming electron to the target ion may occur through non-resonant, background continuum, usually referred to as radiative recombination (RR):



which is the inverse process of direct photoionization, or through the two-step recombination process via autoionizing resonances, i.e. dielectronic recombination (DR):



where the incident electron is in a quasi-bound doubly-excited state which leads either to (i) autoionization, a radiation-less transition to a lower state of the ion and the free electron, or to (ii) radiative stabilization predominantly via decay of the ion core, usually to the ground state, and the bound electron.

In the unified treatment the photoionization cross sections, σ_{PI} , of a large number of low- n bound states – all possible states with $n \leq n_{\max} \sim 10$ – are obtained in the close coupling (CC) approximation as in the Opacity Project (Seaton 1987). Coupled channel calculations for σ_{PI} include both the background and the resonance structures

(due to the doubly excited autoionizing states) in the cross sections. The recombination cross section, σ_{RC} , is related to σ_{PI} , through detailed balance (Milne relation) as

$$\sigma_{RC}(\epsilon) = \frac{\alpha^2}{4} \frac{g_j}{g_i} \frac{(\epsilon + I_p)^2}{\epsilon} \sigma_{PI} \quad (4)$$

in Rydberg units; g_i and g_j are the statistical weight factors of the recombining (target or residual) and recombined ions respectively; α is the fine structure constant, ϵ is the photoelectron energy, and I_p is the ionization potential. In the present work, it is assumed that the recombining ion is in the ground state, and recombination can take place into the ground or any of the excited recombined (e+ion) states. The contributions of these bound states to the total σ_{RC} are obtained by summing over the contributions from individual cross sections. σ_{RC} thus obtained from σ_{PI} , including the autoionizing resonances, corresponds to the total (DR+RR) unified recombination cross section.

Recombination into the high- n states, i.e. $n_{\max} < n \leq \infty$, must also be included (Fig. 1 of NP1). To each excited threshold $S_i L_i (J_i) \pi_i$ of the N -electron target ion, there corresponds an infinite series of $(N+1)$ -electron states, $S_i L_i (J_i) \pi_i \nu \ell$, to which recombination can occur, where ν is the effective quantum number. For these states DR dominates the recombination process and the background recombination is negligibly small. The contributions from these states are added by calculating the collision strengths, Ω_{DR} , employing the precise theory of radiation damping by Bell & Seaton (1985). Several aspects related to the application of the theory to the calculation of DR collision strengths are described in the references cited.

The total (e + ion) recombination rate coefficients may be calculated using the photoionization cross sections $\sigma_{PI}(\epsilon)$ and the DR collision strengths Ω_{DR} . In the present work however, we confine ourselves to a calculation of the level-specific $\sigma_{RC}(T; i \rightarrow j)$, where j refer to the ground state fine structure levels $^3P_{2,0,1}$. The corresponding Maxwellian averaged rate coefficients are obtained as

$$\alpha_{RC}(T; i \rightarrow j) = \frac{g_j}{g_i} \frac{2}{kTc\sqrt{2\pi m^3 kT}} \times \int_0^\infty E^2 \sigma_{PI}(\epsilon; j \rightarrow i) e^{-\epsilon/kT} d\epsilon, \quad (5)$$

where $E = h\nu = \epsilon + I_p$ is the photon energy.

3 COMPUTATIONS

3.1 Residual ion representation for Fe XX

Close coupling calculations for an (e + ion) system require an accurate wavefunction expansion for the states of interest in the target or the residual ion. Donnelly *et al.* (1999) used an elaborate CI representation for the Fe XX states obtained using the atomic structure code CIV3 (Hibbert 1975). We obtain a very similar CI target expansion using the SUPERSTRUCTURE program (Eissner *et al.* 1974), with the same target states as Donnelly *et al.*, i.e. the ones dominated by configurations $2s^2 2p^3$, $2s 2p^4$, $2p^5$, $2s^2 2p^2 3s$ and all associated terms and fine structure levels. Both the CIV3 and the SUPERSTRUCTURE are carried out in intermediate coupling using the Breit-Pauli approximation. Table 1 presents the fine-structure level energies from the present

Table 1. Calculated (cal) LSJ energy levels of Fe XX in Rydbergs and comparison with the observed (obs) energies from NIST (1985), and with those (DBK) by Donnelly *et al.* (1999).

i	Level		E_{cal} (LSJ)	E_{obs}	E (DBK)
1	$2s^2 2p^3 \ ^4S^o$	3/2	0.0000	0.0000	0.0000
2	$2s^2 2p^3 \ ^2D^o$	3/2	1.2789	1.2632	1.2887
3	$2s^2 2p^3 \ ^2D^o$	5/2	1.6446	1.6050	1.6612
4	$2s^2 2p^3 \ ^2P^o$	1/2	2.3700	2.3718	2.3881
5	$2s^2 2p^3 \ ^2P^o$	3/2	2.9332	2.9465	2.9616
6	$2s 2p^4 \ ^4P$	5/2	6.8499	6.8594	6.8674
7	$2s 2p^4 \ ^4P$	3/2	7.4451	7.4799	7.4657
8	$2s 2p^4 \ ^4P$	1/2	7.6432	7.6796	7.6629
9	$2s 2p^4 \ ^2D$	3/2	9.5480	9.5006	9.5729
10	$2s 2p^4 \ ^2D$	5/2	9.6762	9.6445	9.7304
11	$2s 2p^4 \ ^2S$	1/2	10.9215	10.8920	10.9652
12	$2s 2p^4 \ ^2P$	3/2	11.3899	11.3219	11.4352
13	$2s 2p^4 \ ^2P$	1/2	12.2595	12.2113	12.3052
14	$2p^5 \ ^2P^o$	3/2	17.8936	17.8109	17.9667
15	$2p^5 \ ^2P^o$	1/2	18.8721	18.7922	18.9503
16	$2s^2 2p^2 3s \ ^4P$	1/2	65.8494	–	65.3888
17	$2s^2 2p^2 3s \ ^4P$	3/2	66.3955	–	65.9709
18	$2s^2 2p^2 3s \ ^4P$	5/2	66.7934	–	66.3752
19	$2s^2 2p^2 3s \ ^2P$	1/2	66.6709	–	66.2395
20	$2s^2 2p^2 3s \ ^2P$	3/2	67.0759	–	66.4774
21	$2s^2 2p^2 3s \ ^2D$	5/2	67.9909	–	67.5913
22	$2s^2 2p^2 3s \ ^2D$	3/2	68.0771	–	67.6739
23	$2s^2 2p^2 3s \ ^2S$	1/2	69.4502	–	68.7533

BPRM calculation, which are almost identical to those from the SUPERSTRUCTURE results, together with experimental energies (Sugar & Corliss 1985) and those calculated by Donnelly *et al.* using CIV3. The present calculated energies in Table 1 are taken after intermediate coupling stage for the target ion in the code RECUPD of the BPRM package of codes (Scott and Taylor 1982, Hummer *et al.* 1993, Berrington *et al.* 1995). As is readily seen, the agreement between the calculated and observed energies is very good, better than 1% for most of the levels (the present calculated energies are slightly better in agreement with experiment than those of Donnelly *et al.*) Table 2 presents a subset of the oscillator strengths calculated, for the transition array $2s^2 2p^3 \rightarrow 2s 2p^4$, and compared with those of Donnelly *et al.*, and from the U.S. National Institute for Standards and Technology (NIST) compilation by Fuhr *et al.* (1988) based on the relativistic calculations by Cheng *et al.* (1979). All three sets of oscillator strengths are in good agreement; the present values are in somewhat better agreement with the NIST tabulation than Donnelly *et al.* for some transitions. We may therefore deduce that the wavefunction representations in the two calculations, Donnelly *et al.* and ours, are of the same accuracy.

3.2 Photoionization

The BPRM method as applied to self-consistent photoionization and recombination calculations has been discussed in detail in several previous works and references therein (e.g. ZNP, Pradhan & Zhang 1998). The use of such data to astrophysical applications in photoionization modeling, and photoionization and recombination data for all ions of carbon, nitrogen, and oxygen are described by Nahar & Prad-

Table 2. Dipole oscillator strengths (≥ 0.0001) for fine structure transitions in the transition array $2s^2 2p^3 \rightarrow 2s 2p^4$ for the target ion Fe XX; comparisons are with the NIST data by Cheng *et al.* (in Fuhr *et al.* 1988), and with those (DBK) by Donnelly *et al.* (1999).

Transition		Present	NIST	DBK
$^4S^o_{3/2}$	– $^4P_{1/2}$	0.0208	0.0221	0.0208
	– $^4P_{3/2}$	0.0392	0.0413	0.0391
	– $^4P_{5/2}$	0.0503	0.0520	0.0485
	– $^2S_{1/2}$	0.0009	0.0010	0.0011
	– $^2P_{3/2}$	0.0040	0.0045	0.0045
	– $^2D_{3/2}$	0.0021	0.0026	0.0028
$^2P^o_{1/2}$	– $^4P_{1/2}$	0.0010	0.0011	0.0012
	– $^2S_{1/2}$	0.0622	0.0640	0.0615
	– $^2P_{1/2}$	0.0057	0.0057	0.0045
	– $^2P_{3/2}$	0.0272	0.0284	0.0279
	– $^2D_{3/2}$	0.0141	0.0146	0.0130
	$^2P^o_{3/2}$	– $^4P_{3/2}$	0.0010	0.0011
– $^4P_{5/2}$		0.0003	0.0003	0.0003
– $^2S_{1/2}$		0.0026	0.0030	0.0018
	– $^2P_{1/2}$	0.0679	0.0700	0.0677
	– $^2P_{3/2}$	0.0169	0.0167	0.0162
	– $^2D_{3/2}$	0.0018	0.0020	0.0016
$^2D^o_{3/2}$	– $^2D_{5/2}$	0.0242	0.0250	0.0236
	– $^4P_{1/2}$	0.0004	0.0005	0.0005
	– $^4P_{3/2}$	0.0003	0.0004	0.0003
	– $^4P_{5/2}$	0.0033	0.0038	0.0041
	– $^2S_{1/2}$	0.0289	0.0300	0.0297
	– $^2P_{1/2}$	0.0148	0.0151	0.0132
$^2D^o_{5/2}$	– $^2P_{3/2}$	0.0187	0.0181	0.0159
	– $^2D_{3/2}$	0.0742	0.0780	0.0745
	– $^4P_{3/2}$	0.0001	0.0001	0.0002
	– $^4P_{5/2}$	0.0011	0.0012	0.0013
	– $^2P_{3/2}$	0.0868	0.0890	0.0853
	– $^2D_{5/2}$	0.0599	0.0630	0.0589

han (1998) and Nahar (1999). Donnelly *et al.* also provide a detailed discussion of the R-matrix method and the calculations. In the present work we confine the calculations to the ground term levels considered by Donnelly *et al.* for both the total and partial photoionization cross sections.

In addition to the BPRM calculations using the target expansion described in the above sub-section, non-relativistic LS coupling calculations, using the same target, were carried out for comparison. We also obtained two other data sets for the photoionization of Fe XIX, with the relativistic distorted wave (RDW) code (Zhang 1998), and with the semi-relativistic atomic structure code CATS (Abdallah *et al.* 1988) and ionization code GIPPER (Clark & Abdallah, unpublished) of the Los Alamos National Laboratory (LANL).

3.3 Recombination rate coefficients

Maxwellian averaged recombination rate coefficients for the ground term levels $2s^2 2p^4 \ ^3P_{2,0,1}$ are obtained using the partial photoionization cross sections σ_{PI} for the transitions $h\nu + 2s^2 2p^4 \ (^3P_J) \rightarrow e + 2s^2 2p^3 \ (^4S^o_{3/2})$. The recombination rates were also calculated using the LS coupling photoionization cross sections for $h\nu + 2s^2 2p^4 \ (^3P) \rightarrow e + 2s^2 2p^3 \ (^4S^o)$, for comparison with the relativistic calculations.

3.4 Oscillator strengths

Another indication of the accuracy of the bound-free photoionization calculations may be obtained by calculating the bound-bound radiative transition probabilities using the BPRM method for the fine structure E1 (dipole allowed and intercombination) transitions (e.g. Nahar and Pradhan 1999a,b). As the same bound state wavefunction expansions are employed in both the bound-free and the bound-bound transitions, one expects the same accuracy. A number of oscillator strengths of Fe XIX were computed and compared with other accurate calculations using the multiconfiguration Dirac-Fock (MCDF) method by Cheng *et al.* (1979).

4 RESULTS AND DISCUSSION

Results for photoionization, recombination, and transition probabilities calculated in the present work are consistent with one another, as discussed below.

4.1 Photoionization cross sections

Fig. 1 presents the total photoionization cross sections for the three ground term fine structure levels $^3P_{2,0,1}$ using the BPRM method (the solid lines) and the RDW method (the dashed lines). The non-relativistic LS coupling photoionization cross sections of the 3P term and the weighted average of the RDW results are also presented (Fig. 1d). Comparing our Fig. 1 with Figs. 1 and 2 in Donnelly *et al.* one sees the present BPRM results differ considerably with those by Donnelly *et al.* in the following three aspects: 1) while the results of Donnelly *et al.* exhibit large variations in the background cross sections for the three levels, the present BPRM results show those to be nearly the same; 2) in the photon energy range $\sim 126 - 154$ Ry, the cross sections for levels 3P_2 and 3P_1 in Donnelly *et al.*'s Fig. 1 show extensive and strong resonance structures while our results do not; 3) the weighted average (not shown directly here) of the background cross sections for the three fine structure levels in our results would be very close to the non-relativistic LS results, as is obvious from Fig. 1, while those in Donnelly *et al.* differ from the non-relativistic LS values by more than a factor of two.

However, the detailed resonance structures in the present BPRM calculations are more extensive and differ significantly from the LS calculations. Fig. 2 shows the cross sections at higher resolution. It is apparent that the resonance positions in the LS 3P results (panel d) do not correspond in detail or magnitude to the individual resonances in the cross sections for the fine structure components $^3P_{2,0,1}$ (panels a,b,c respectively).

Fig. 3 presents the partial cross sections for photoionization from the ground level 3P_2 of Fe XIX into a few fine structure levels of the residual ion Fe XX. Comparing this figure with Fig. 3 in Donnelly *et al.*, one again sees that similar significant differences exist in both the background and the resonances, especially the resonances in the photoelectron energy region 20 – 45 Ry.

Now we discuss the above three major differences between the present results and those in Donnelly *et al.* 1) From our many other calculations, such as those shown in

Fig. 1 for Fe XXII and Figs. (4c) and (4d) for Fe XXIV in Zhang (1998), the relativistic effects do not appear to affect the background photoionization cross sections very much, and the backgrounds for the fine structure levels corresponding to the same energy term appear to be almost the same. Those BPRM results, as well as the present results, were all confirmed by the RDW calculations (shown as dotted or dashed lines in the corresponding figures). The backgrounds in the present BPRM results also agree with the semi-relativistic results from the LANL codes (basically similar to the RDW results and therefore not shown). 2) The resonances in the photon energy region $\sim 126 - 154$ Ry, or the photoelectron energy region $\sim 20 - 45$ Ry, obtained by Donnelly *et al.* would correspond to the process

$$h\nu + 2s^22p^4 \rightarrow 2\ell^43\ell n'\ell \rightarrow 2s^22p^3 + e, \quad (6)$$

with $n' \geq 3$; it is obvious that the first step in this process involves two-electron jumps and is not allowed (there would be some contributions through the configuration mixing among the $n = 2$ and 3 states but these would not produce such strong resonances). 3) As is clear from the discussion in 1), the background in the weighted average of the results for the three levels should not differ much from the non-relativistic LS-coupling results. This should be true for ions with low and intermediate nuclear charge Z , where the relativistic effect should not be significant enough to affect the background. Indeed, we usually use this fact to check our calculations.

The detailed resonance structures on the other hand may differ considerably since they correspond to different target thresholds in the BPRM and the LS coupling calculations. In the relativistic calculations the Rydberg series of resonances are more extensive owing to the many more fine structure level splittings in the target than the LS terms.

We also note that a preliminary set of BPRM calculation with a smaller number of target terms, excluding the $2s^22p^23s$, also yielded essentially the same results for the photoionization cross sections. This is expected for highly charged ions since the configuration interaction between different n-complexes decreases with ion charge.

4.2 Recombination rate coefficients

Table 3 presents the $\alpha_R(T)$ calculated using the σ_{RC} obtained from the partial photoionization cross sections $\sigma_{PI}(^3P_J \rightarrow ^4S_{3/2}^o)$, for the three levels $J = 2, 0, 1$. The sum of the recombination rate coefficients for these three fine structure levels is also given, together with the LS coupling results. It is important to note that the total recombination rate coefficient into a LS term is a *simple sum* of the values for the individual fine structure levels corresponding to this term. This is because the expression for the recombination rate (see our Eq. (5) or Eq. (7) in Donnelly *et al.*) already includes a multiplication by the statistical weight factor, which is $g_j = (2J + 1)$ in our Eq. (5) and ω_j in Donnelly *et al.*'s Eq. (7). We note that, as shown by Eq. (3) of NP2, the *total* recombination rate coefficient for a given target level is obtained by *summing* over contributions from all possible states or levels in the recombined ion. Donnelly *et al.*, on the other hand, performed a “weighted average” in order to obtain the recombination rate coefficient for the LS term – leading to a further error in their numerical values

Table 3. The present BPRM recombination rates as functions of temperature for the transitions from the ground level $2s^22p^3\ ^4S_{3/2}^o$ in Fe XX to the three levels of Fe XIX in its ground term $2s^22p^4\ ^3P_J$; the sum of the values for these levels (SUM) is also shown and compared with the non-relativistic LS-coupling results (LS).

T(K)	3P_2	3P_0	3P_1	SUM	LS
5.0[4]	2.57[-11]	4.24[-12]	1.11[-11]	4.11[-11]	2.78[-11]
6.0[4]	2.31[-11]	3.99[-12]	1.03[-11]	3.74[-11]	2.57[-11]
7.0[4]	2.12[-11]	3.77[-12]	9.63[-12]	3.46[-11]	2.39[-11]
8.0[4]	1.96[-11]	3.55[-12]	9.06[-12]	3.22[-11]	2.24[-11]
9.0[4]	1.83[-11]	3.36[-12]	8.55[-12]	3.02[-11]	2.10[-11]
1.0[5]	1.71[-11]	3.18[-12]	8.09[-12]	2.84[-11]	1.98[-11]
2.0[5]	1.04[-11]	2.01[-12]	5.15[-12]	1.75[-11]	1.25[-11]
3.0[5]	7.44[-12]	1.45[-12]	3.75[-12]	1.26[-11]	9.15[-12]
4.0[5]	5.81[-12]	1.13[-12]	2.94[-12]	9.88[-12]	7.24[-12]
5.0[5]	4.77[-12]	9.33[-13]	2.43[-12]	8.12[-12]	6.01[-12]
6.0[5]	4.05[-12]	7.93[-13]	2.07[-12]	6.91[-12]	5.16[-12]
7.0[5]	3.52[-12]	6.90[-13]	1.80[-12]	6.01[-12]	4.54[-12]
8.0[5]	3.12[-12]	6.12[-13]	1.60[-12]	5.33[-12]	4.06[-12]
9.0[5]	2.80[-12]	5.50[-13]	1.43[-12]	4.79[-12]	3.68[-12]
1.0[6]	2.55[-12]	5.01[-13]	1.30[-12]	4.35[-12]	3.38[-12]
2.0[6]	1.38[-12]	2.70[-13]	6.98[-13]	2.34[-12]	1.94[-12]
3.0[6]	9.63[-13]	1.89[-13]	4.86[-13]	1.64[-12]	1.41[-12]
4.0[6]	7.43[-13]	1.45[-13]	3.73[-13]	1.26[-12]	1.11[-12]
5.0[6]	6.03[-13]	1.18[-13]	3.02[-13]	1.02[-12]	9.12[-13]
6.0[6]	5.04[-13]	9.84[-14]	2.52[-13]	8.54[-13]	7.70[-13]
7.0[6]	4.30[-13]	8.40[-14]	2.15[-13]	7.29[-13]	6.62[-13]
8.0[6]	3.73[-13]	7.29[-14]	1.86[-13]	6.32[-13]	5.78[-13]
9.0[6]	3.28[-13]	6.40[-14]	1.63[-13]	5.55[-13]	5.10[-13]
1.0[7]	2.91[-13]	5.69[-14]	1.45[-13]	4.93[-13]	4.54[-13]

– and found a different kind of discrepancy compared with the LS coupling results.

The present rate coefficients for the 3P term obtained by summing over the fine structure values are also significantly higher than the LS coupling results, especially for the low temperatures, the BPRM results being larger by up to 50%. In contrast, the BPRM results in Donnelly *et al.* are up to a factor of 2 smaller than the LS values. The differences between the BPRM and the LS coupling values in the present results are due to the different details of the resonance structures in the two cases. Whereas in LS coupling the fine structure thresholds belonging to a given LS term are degenerate, these are explicitly included in the BPRM calculations at the appropriate energies and consequently the resonances are more numerous. As displayed earlier in Fig. 2, the resonance positions and shapes are also different in the BPRM and LS coupling calculations. Further, more levels of the autoionizing terms which do not autoionize in the LS coupling case contribute in the BPRM case (for example, see the discussion on the $1s2p3p$ autoionizing states in Sec. IIIB in Zhang (1998)). At higher temperatures the differences between the present LS coupling and BPRM rates are smaller, since the overall background cross sections are of similar magnitude at higher energies, above all $n = 2$ target thresholds. It might also be pointed out that the autoionizing resonances are unlikely to be significantly dampened due to radiative decays, to affect the overall cross sections and rates, since they involve $\Delta n = 0$ transitions with much smaller radiative rates than autoionization rates.

Table 4. Dipole oscillator strengths for fine structure transitions in the transition array $2s^22p^4\ ^3P \rightarrow 2s2p^5\ ^{3,1}P^o$ for Fe XIX; comparisons are with the NIST data by Cheng *et al.* (in Fuhr *et al.* 1988)

Transition	Present	NIST
$^3P_2 - ^3P_1^o$	0.129	0.147
$- ^1P_1^o$	0.0313	0.0355
$- ^3P_2^o$	0.296	0.34
$^3P_0 - ^3P_1^o$	0.0772	0.087
$- ^1P_1^o$	0.0037	0.005
$^3P_1 - ^3P_0^o$	0.0898	0.1035
$- ^3P_1^o$	0.0617	0.0705
$- ^1P_1^o$	0.0029	0.003
$- ^3P_2^o$	0.0986	0.1122

Further discussion of recombination theory in the close coupling formulation, including the R-matrix method, is given in several previous works: Davies and Seaton (1969), Bell and Seaton (1985), Robicheaux *et al.* (1995), Gorczyca and Badnell (1997), Pradhan and Zhang (1997), Badnell *et al.* (1998), Robicheaux (1998), Seaton (1998), and Zhang *et al.* (1999).

4.3 Transition Probabilities

Transition probabilities provide an independent test of the accuracy of the bound state wavefunctions. Fine structure transition probabilities may be computed for E1 dipole allowed and intercombination transitions using recent developments in the BPRM method (Hummer *et al.* 1993, Berrington *et al.* 1998, Nahar and Pradhan, 1999a,b). We calculate the oscillator strengths for the fine structure components within several multiplets corresponding to the initial 3P symmetry and final $^{3,1}(S, P, D)^o$ symmetries. Table 4 presents a subset of these results: the gf-values for the transitions $2s^22p^4\ ^3P_{2,0,1} \rightarrow 2s2p^5\ ^{3,1}P_{1,2}^o$. The present results are compared with the MCDF calculations by Cheng *et al.* (1979) that have been incorporated in the evaluated compilation by the U.S. National Institute of Standards and Technology (NIST; Fuhr *et al.* 1988). In all cases the agreement between the present BPRM results and the MCDF values is within about 10%. Both the length and the velocity oscillator strengths are obtained, and found to be in good agreement for the stronger transitions ($gf > 0.01$) in all multiplets calculated.

ACKNOWLEDGMENTS

The work by HLZ was performed under the auspices of the US Department of Energy. The work by AKP was partially supported by grants from the US National Science Foundation (AST-9870089) and NASA (NAG5 6908). The computational work was carried out at the Ohio Supercomputer Center in Columbus Ohio.

REFERENCES

Abdallah, J. Jr., Clark, R.E.H., & Cowan, R.D., 1988. Los Alamos Manual LA-11436-MIV

- Badnell, N.R., Gorczyca, T.W. and Price, A.D., 1998, *Journal Of Physics B*, 31 L239
- Bell, R.H. & Seaton, M.J., 1985. *Journal Of Physics B*, 18, 1589
- Berrington, K.A., J. Pelan, and L. Quigley, 1998, *Physica Scripta*, 57, 549
- Berrington, K.A., Eissner, W., Norrington, P.H., 1995, *Comput. Phys. Commun.*, 92, 290
- Cheng, K.T., Kim, Y.K. & Desclaux, J.P., 1979, *At. Data Nucl. Data Tables*, 24, 1111
- Davies, P.C.W. and Seaton M.J. 1969 *Journal Of Physics B*, 2, 757
- Donnelly, D., Bell, K.L. & Keenan, F.P, 1999. *MNRAS*, 307, 595
- Eissner, W., Jones M. & Nussbaumer, H. 1974. *Comput. Phys. Commun.*, 8, 270
- Fuhr, J.R., Martin, G.A. & Wiese, W.L., 1988. *J. Phys. Chem. Ref. Data* 17, Suppl No. 4 (NIST)
- Gorczyca, T.W. and Badnell, N.R., 1997, *Physical Review Letters*, 79, 2783
- Hibbert, A., 1975. *Comput. Phys. Commun.* 9, 141
- Hummer, D.G., Berrington, K.A., Eissner, W., Pradhan, A.K., Saraph, H.E. & Tully, J.A., 1993. *Astron. Astrophys.*, 279, 298
- Liedahl, D.A., Kahn, S.M., Osterheld, A.L. & Goldstein, W.H., 1992. *Astrophys. J.*, 391, 306
- Nahar, S.N. 1999. *Astrophys. J. Suppl. Ser.*, 128, 131
- Nahar, S.N. & Pradhan, A.K., 1992, *Physical Review Letters*, 68, 1488 (NP1)
- Nahar, S.N. & Pradhan, A.K., 1994, *Physical Review A*, 49, 1816 (NP2)
- Nahar, S.N. & Pradhan, A.K., 1998, *Astrophys. J. Suppl. Ser.*, 111, 339
- Nahar, S.N. & Pradhan, A.K., 1999a, *Astron. Astrophys. Suppl.*, 135, 347
- Nahar, S.N. & Pradhan, A.K., 1999b, *Physica Scripta* (submitted)
- Pradhan, A.K. & Zhang, H.L., 1997, *Journal Of Physics B*, 30, L571
- Robicheaux, F. 1998, *Journal Of Physics B*, 31, L109
- Robicheaux, F., Gorczyca, T.W., Pindzola, M.S. and Badnell, N.R., 1995, *Physical Review A*, 52, 1319
- Scott, N.S. and Taylor, K.T., 1982, *Comput. Phys. Commun.*, 25, 347
- Seaton, M.J., 1998, *Journal Of Physics B*, 31, L1017
- Sugar, J. & Corliss, C., 1985, *J. Phys. Chem. Ref. Data* 14, Suppl. 2
- Zhang, H.L., 1998. *Physical Review A*, 57, 2640
- Zhang, H.L., Nahar, S.N. & Pradhan, A.K., 1999. *Journal Of Physics B*, 32, 1459
- Zhang, H.L. & Pradhan, A.K., 1997. *Physical Review Letters*, 78, 195

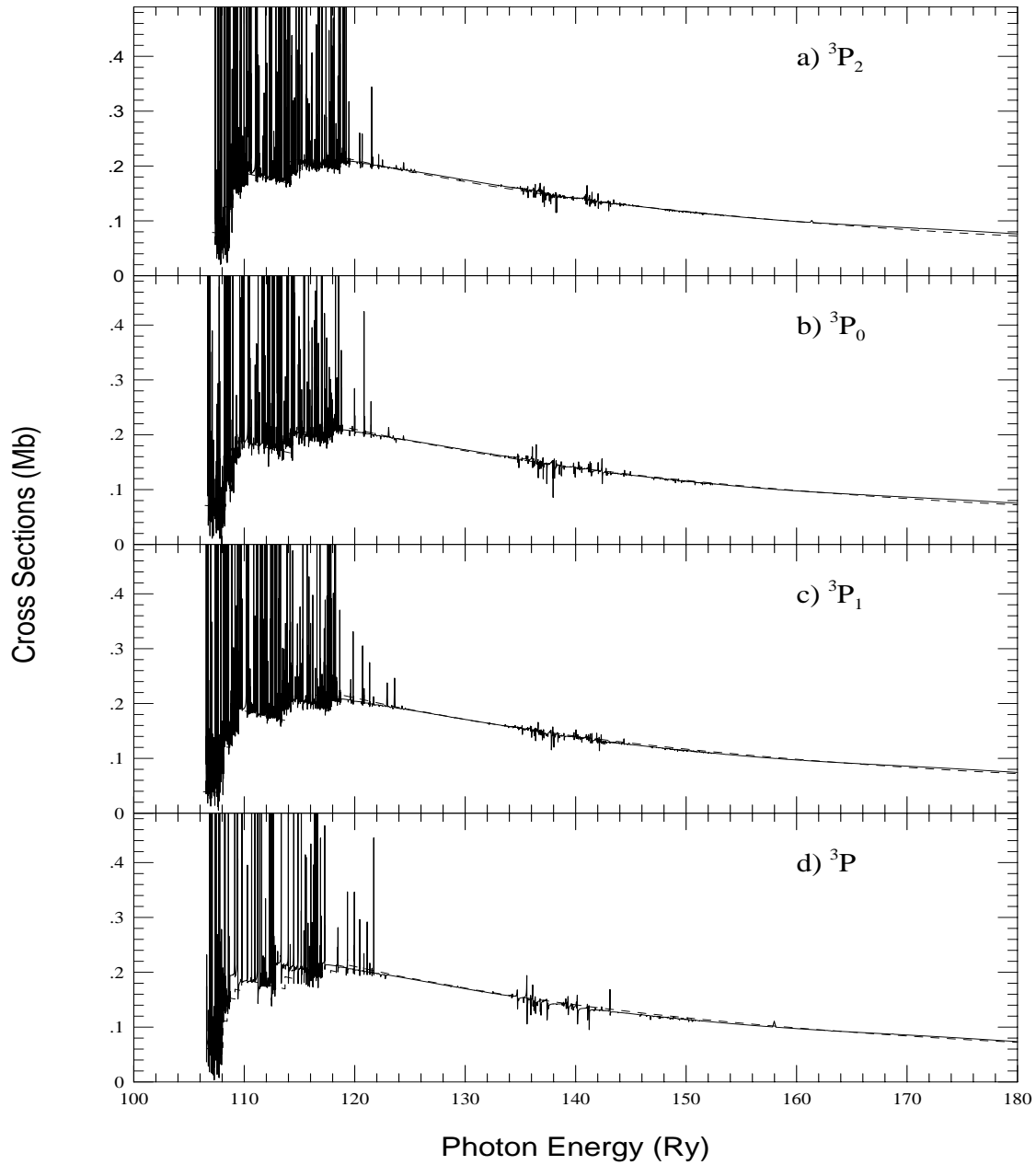


Figure 1. Total photoionization cross sections for the three levels $J = 2, 0, 1$ (a, b and c) of the ground term $2s^2 2p^4 \ ^3P$ in Fe XIX by the present BPRM (solid lines) and the RDW (dashed lines) calculations. The non-relativistic LS coupling results are also presented (d), together with the average values of the RDW results (the dashed line).

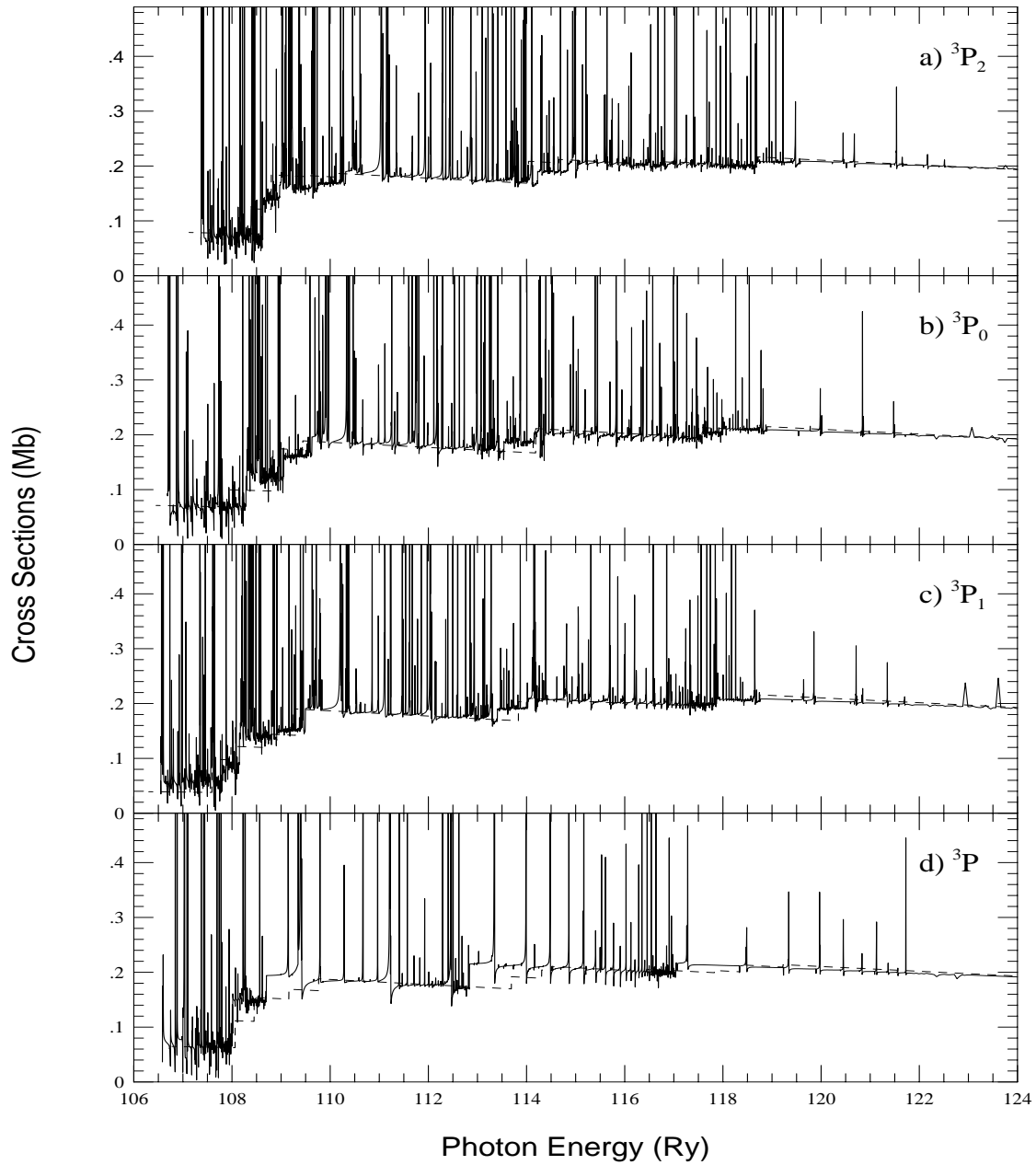


Figure 2. As in Fig. 1, but with resonance structures at high-resolution.

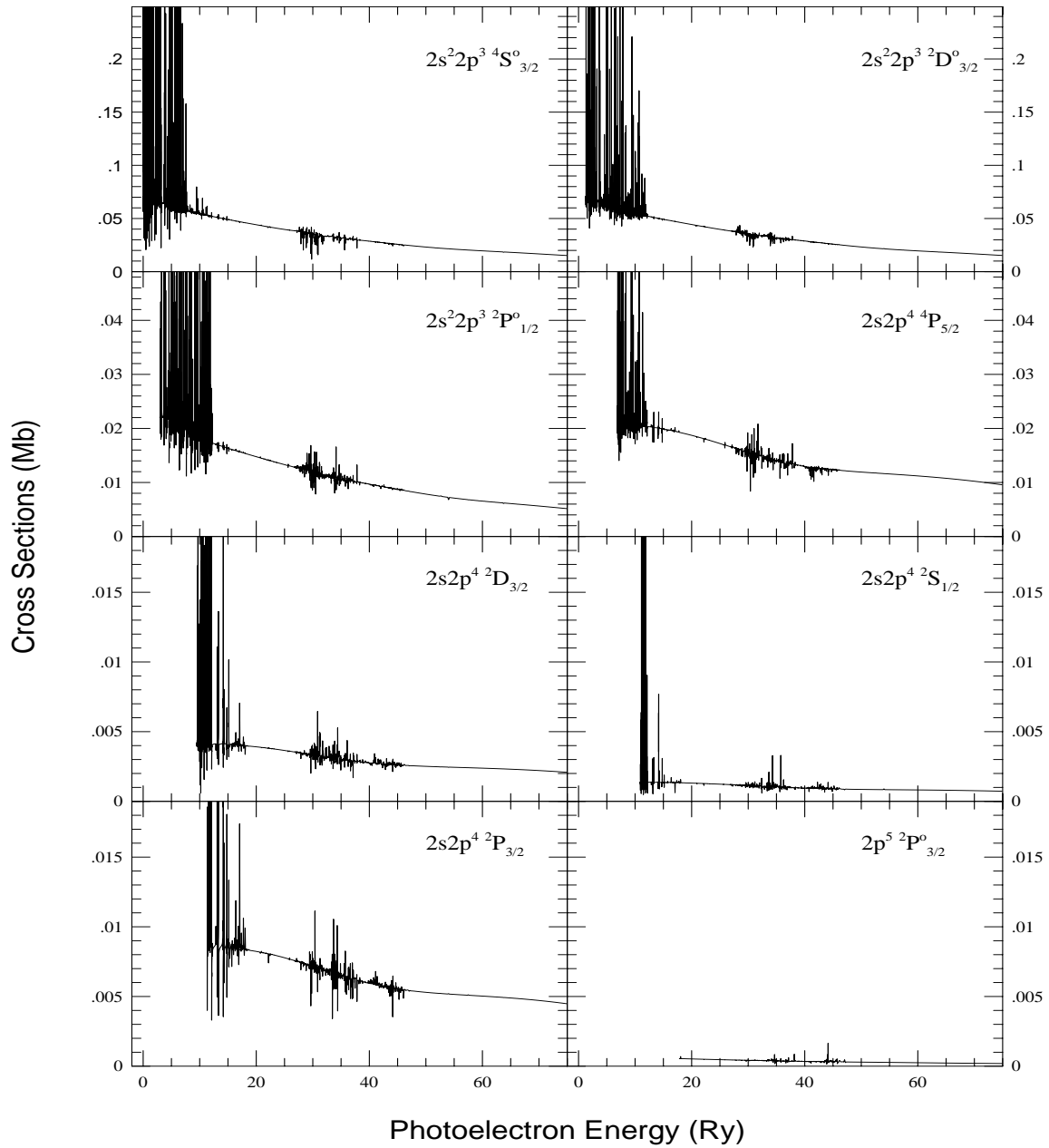


Figure 3. Partial photoionization cross sections for the transitions from the ground level $2s^2 2p^4 \ ^3P_2$ in Fe XIX to one of the low-lying levels in the residual ion Fe XX by the present BPRM calculation.